THE JOURNAL OF BIOLOGICAL CHEMISTRY VOL. 284, NO. 44, pp. 30604–30614, October 30, 2009

Aberrant DNA Polymerase α Is Excluded from the Nucleus by Defective Import and Degradation in the Nucleus*[S]

Received for publication, May 26, 2009, and in revised form, August 19, 2009 Published, JBC Papers in Press, September 2, 2009, DOI 10.1074/jbc.M109.024760

Christian S. Eichinger[‡1], Takeshi Mizuno[‡§¶2], Keiko Mizuno[¶], Yasuyuki Miyake[‡3], Ken-ichiro Yanagi[‡¶], Naoko Imamoto[¶], and Fumio Hanaoka[‡§‖4]

From the [‡]Cellular Physiology Laboratory and [¶]Cellular Dynamics Laboratory, Advanced Science Institute, RIKEN, and [§]SORST, Japan Science and Technology Corporation, Wako, Saitama 351-0198 and the [‖]Graduate School of Frontier Biosciences, Osaka University, Suita, Osaka 565-0871, Japan

DNA polymerase α is essential for the onset of eukaryotic DNA replication. Its correct folding and assembly within the nuclear replication pre-initiation complex is crucial for normal cell cycle progression and genome maintenance. Due to a single point mutation in the largest DNA polymerase α subunit, p180, the temperature-sensitive mouse cell line tsFT20 exhibits heat-labile DNA polymerase α activity and S phase arrest at restrictive temperature. In this study, we show that an aberrant form of endogenous p180 in tsFT20 cells (p180^{tsFT20}) is strictly localized in the cytoplasm while its wild-type counterpart enters the nucleus. Time-lapse fluorescence microscopy with enhanced green fluorescent protein-tagged or photoactivatable green fluorescent protein-tagged p180^{tsFT20} variants and inhibitor analysis revealed that the exclusion of aberrant p180^{tsFT20} from the nucleus is due to two distinct mechanisms: first, the inability of newly synthesized (cytoplasmic) p180^{tsFT20} to enter the nucleus and second, proteasome-dependent degradation of nuclear-localized protein. The nuclear import defect seems to result from an impaired association of aberrant *de novo* synthesized p180^{tsFT20} with the second subunit of DNA polymerase α, p68. In accordance, we show that RNA interference of p68 results in a decrease of the overall p180 protein level and in a specific increase of cytoplasmic localized p180 in NIH3T3 cells. Taken together, our data suggest two mechanisms that prevent the nuclear expression of aberrant DNA polymerase α.

The highly conserved DNA polymerase α-primase complex is the only eukaryotic polymerase that can initiate DNA synthesis *de novo*. Thus, its recruitment is a crucial step in the tightly regulated stepwise assembly of the replication machinery in eukaryotic cells. This complex is required for the synthesis of RNA primers, an essential prerequisite for the initiation of replication, and for the discontinuous synthesis of Okazaki fragments on the lagging strand (1–4). Moreover, DNA polymerase α plays a fundamental role in coordinating DNA replication, DNA repair, and cell cycle progression (1), in telomere capping and length regulation (5–9), and in the epigenetic control of transcriptional silencing and nucleosome reorganization (10, 11).

The DNA polymerase α-primase complex consists of four subunits, each of which is conserved in eukaryotes; in yeast, all four subunits are essential for viability (2). The largest subunit, 180 kDa (p180), harbors the catalytic polymerase α activity. The two smallest subunits, 54 kDa (p54) and 46 kDa (p46), provide primase activity. The p46 protein, which is coupled to p180 by p54, synthesizes RNA primers and is involved in regulating their length; it also functions in cell cycle checkpoints (12). The 68-kDa subunit (p68) plays a crucial regulatory role in the early stage of chromosomal replication in yeast and has been shown to be essential for the nuclear import of p180 in mouse cells (13, 14).

DNA replication takes place during a restricted period in the cell cycle, in the S phase. To avoid errors in DNA duplication that compromise genome integrity in vertebrate cells, the transition from G_1 to S phase and the onset of DNA polymerase activity are highly regulated by at least two cyclin-dependent kinases, cyclin E/cdk2 and cyclin A/cdk2 (15, 16). In an SV40 *in vitro* system, phosphorylation of p68 inhibits replication initiation as well as primer synthesis and elongation (17), and the p180 subunit contains multiple regulatory phosphorylation sites (18, 19). In addition to regulation by phosphorylation, expression of the DNA polymerase α gene is controlled during the cell cycle by E2F, GABP, and Sp1 transcription factors (20, 21). Thus, the activity of DNA polymerase α is tightly controlled at the transcriptional and post-translational levels, whereas less is known about its subcellular distribution, regulation, and behavior under various stress conditions.

The tsFT20 cell line, a temperature-sensitive mutant clone identified in a screen of *N*-methyl-*N*′-nitro-*N*-nitroguanidine-treated mouse mammary carcinoma FM3A cells, has been the subject of several genetic and biochemical studies (22–34). Compared with parental FM3A cells, this cell line grows normally at 33 °C. However, at the restrictive temperature of 39.5 °C, they exhibit a phenotype closely resembling that con-

* This work was supported by grants from the Ministry of Education, Culture, Sports, Science, and Technology of Japan, a grant from the Human Frontier Science Program, grants from the Bioarchitect Research Project and the Chemical Biology Project of RIKEN (to T. M. and N. I.) and the director fund of RIKEN (to T. M.), research fellowships from the Studienstiftung des deutschen Volkes (German National Merit Foundation) (to C. S. E.) and the Center of Excellence (COE) from the Japan Society for the Promotion of Science (to Y. M.).

[S] The on-line version of this article (available at http://www.jbc.org) contains supplemental Movies 1–4 and Figs. S1–S3.

[1] Present address: Max Planck Institute of Biochemistry, Martinsried, Germany.

[2] To whom correspondence should be addressed: Cellular Dynamics Laboratory, Advanced Science Institute, RIKEN, 2-1 Hirosawa, Wako, Saitama 351-0198, Japan. Tel.: 81-48-467-9554; Fax: 81-48-462-4716; E-mail: tmizuno@riken.jp.

[3] Present address: Kyoto University, Kyoto, Japan.

[4] Present address: Gakushuin University, Tokyo, Japan.

ferred by arrest at the G_1/S boundary. At the restrictive temperature, tsFT20 cells were further characterized as defective in DNA replication, with a highly decreased DNA synthesis rate, reduced frequencies of replicon initiation, and extensive chromosome aberrations. Purified DNA polymerase α from tsFT20 cells was found to be temperature-sensitive although composed of the same hetero-tetrameric complex as that of FM3A cells, and this defect was ascribed to a single point mutation that changes amino acid 1180 of the p180 subunit from serine to phenylalanine (28). The abnormal cessation of DNA replication in tsFT20 cells at the restrictive temperature results in cell death via the induction of DNA double strand breaks, suggesting that aberrant DNA polymerase α is cytotoxic and also that in general a specific quality control mechanism for the pool of aberrant DNA polymerase α in wild-type cells may be crucial to ensure genomic stability and accurate DNA replication. Recently, it was reported that in *Saccharomyces cerevisiae*, reduced levels of the replicative DNA polymerase α result in greatly elevated frequencies of chromosome translocations and chromosome loss (35). Similarly, when Mcm10 or Ctf4 are depleted in mammalian cells, DNA polymerase α levels are markedly reduced, suggesting that DNA polymerase α levels are indeed crucially regulated by as yet unknown cellular mechanisms (36, 37).

Misfolded and non-functional proteins must be degraded to assure the correct functioning of cellular processes. Several mechanisms that ensure the removal of defective proteins have been described, the most prominent being ER[5]-associated degradation, a process that governs the degradation of unfolded ER proteins in the cytoplasm (38, 39). Degradation systems that function in quality control have also been identified in the secretory pathway and in mitochondria (40). These processes are carried out by proteasomes, organelles consisting of several proteases that are located in the cytoplasm as well as in the nucleus (41, 42, 43). Moreover, most cystic fibrosis patients inherit at least one mutant allele of the ion channel cystic fibrosis transmembrane regulator, which has a temperature-sensitive folding defect causing its detection by the endoplasmic quality control system (44). In contrast, the degradation-dependent protein quality control mechanisms that act in the nucleus are still poorly understood. Recently, Gardner *et al.* (45) reported that San1-mediated degradation acts as a protein quality control system in *S. cerevisiae* nuclei. However, it is still unclear how aberrant nuclear proteins are recognized by ubiquitin E3 ligases and whether analogous systems exist in higher eukaryotes.

In this study, we observed the subcellular distribution and protein expression of an aberrant form of the endogenously expressed DNA polymerase α subunit p180 in tsFT20 cells ($p180^{tsFT20}$) at the restricted temperature using a specific p180 antibody. Surprisingly, we found that endogenous $p180^{tsFT20}$ was rapidly degraded in the nucleus at the restricted temperature, concomitantly with *de novo* synthesized protein accumulating in the cytoplasm. Based on these crucial findings on endogenous $p180^{tsFT20}$, we transiently expressed GFP-tagged $p180^{tsFT20}$ in NIH3T3 or COS-1 cells and made the very same observation that the aberrant p180 variant is excluded from the nucleus and accumulates in the cytoplasm at the restrictive temperature, whereas the wild-type counterpart normally localizes to the nucleus. Inhibitor studies combined with immunofluorescence analysis suggest two mechanisms that exclude aberrant $p180^{tsFT20}$ from the nucleus: defective nuclear import of *de novo* synthesized protein and proteasome-dependent degradation of nuclear localized protein. Our data further suggests that a single point mutation in $p180^{tsFT20}$ presumably causes conformational changes that alter the hydrophobic character of the protein surface, rendering $p180^{tsFT20}$ unable to bind the p68 subunit, which leads in turn to its inability to enter the nucleus (cytoplasmic fraction) or its recognition by the proteasome-dependent degradation machinery (nuclear fraction). In accordance with this assumption, we find that the knockdown of p68 by RNA interference results in a decrease of the overall p180 protein level and a specific increase of cytoplasmically expressed p180. Our findings thus offer mechanistic insights into how the aberrant DNA polymerase α subunit p180 (and probably other malformed nuclear proteins) are cleared from the nucleus to avoid its inappropriate involvement in DNA replication.

EXPERIMENTAL PROCEDURES

Plasmid Construction—Expression plasmids encoding p180 or p68 were previously described (14). Using the primers tsFT20-s 5′-GTGATACGGTGTTCTATGTTATTTG-3′ and tsFT20-as 5′-CAAATAACATAGAACACCGTATCAC-3′, a specific point mutation that creates the S1180F alteration was inserted in plasmid vectors pSRa-p180, pSRα-p180-GFP, and pSRα-H-core (14, 46) with the PCR-based QuikChange II Site-directed mutagenesis kit (Stratagene, La Jolla, CA). To generate the expression plasmid pSRα-$p180^{tsFT20}$PA-GFP encoding photoactivatable GFP-tagged $p180^{tsFT20}$, four point mutations (L64F, T65S, V163A, and T204H in EGFP) were introduced (47). The p68-mRFP fusion expression plasmid was constructed by fusing mRFP1 cDNA to the C terminus of p68. The identity of each construct was confirmed by sequencing using an Applied Biosystems 3130 automatic DNA sequencer.

Cell Culture, Transfection Techniques, and Addition of Inhibitors—NIH3T3 mouse cells were cultured in a 5% CO_2 incubator in Dulbecco's modified Eagle's medium supplemented with 10% calf serum and used for direct immunofluorescence analysis and time-lapse fluorescence microscopy. For Western blot analysis and co-immunoprecipitation, COS-1 cells were grown in the same medium supplemented with 10% fetal bovine serum instead of calf serum. Mouse FM3A cells and the tsFT20 strain were maintained at the permissive temperature (33 °C) in RPMI 1640 medium supplemented with 10% calf serum. NIH3T3 cells ($1–3 \times 10^4$ cells/well) were kept at 37 °C for 16 h and transfected in 8-well chamber slides (Nunc) using Lipofectamine (Invitrogen) or transfectin (Bio-Rad) according to the manufacturer's instructions. COS-1 cells were transfected using FuGENE 6 reagent (Roche). If not otherwise men-

[5] The abbreviations used are: ER, endoplasmic reticulum; GFP, green fluorescent protein; LMB, leptomycin B; CHX, cycloheximide; PA-GFP, photoactivatable green fluorescent protein; mRFP, mouse red fluorescent protein; CSK, cytoskeleton buffer; PIPES, 1,4-piperazinediethanesulfonic acid; siRNA, small interfering RNA.

tioned, transfected cells were incubated in appropriate media for 48 h at 33 °C and then kept at 33 °C or shifted to 39.5 °C. The inhibitors leptomycin B (LMB) (2.5 nM, Sigma), MG132 (5 μM, Calbiochem), and cycloheximide (CHX) (0.1 mM, Aldrich) were added 1 h before the temperature shift, if not otherwise mentioned.

Preparation of Cell Extracts—Following transfection, COS-1 cells were washed twice with phosphate-buffered saline, scraped from plates into ice-cold phosphate-buffered saline, centrifuged (3000 × *g*, 5 min, 4 °C) and frozen as pellets at −80 °C. After thawing, the cells were resuspended in cytoskeleton buffer (CSK) (10 mM PIPES, pH 6.8, 300 mM sucrose, 100 mM NaCl, 3 mM $MgCl_2$, 1 mM EGTA) supplemented with a protease inhibitor mixture (Roche), 0.2 mg/ml phenylmethylsulfonyl fluoride, 1 mM dithiothreitol, and 0.1% Triton X-100 for 1 h at 4 °C, and centrifuged (3000 × *g*, 5 min, 4 °C). The supernatant (S1 fraction) was collected and the insoluble chromatin fraction was further extracted with the same solution as above but supplemented with 0.3 M KCl, incubated for 30 min at 4 °C, and separated by centrifugation (3000 × *g*, 5 min, 4 °C). Again, the supernatant was collected (S3 fraction) and the remaining insoluble material (pellet fraction) was dissolved in 70 μl of SDS sample buffer. The tsFT20 cells were incubated at permissive (33 °C) or restrictive (39.5 °C) temperatures for the indicated times, harvested by centrifugation, and resuspended in SDS sample buffer.

Western Blot Analysis—For Western blot analysis, the S1 or the pellet fraction was subjected to 8% SDS-PAGE and transferred to a 0.45-μm polyvinylidene difluoride membrane (Millipore). The membranes were washed three times (5 min at room temperature) with TBSSM buffer (50 mM Tris-HCl, pH 7.5, and 150 mM NaCl), blocked with 5% skim milk (30 min at room temperature), incubated with primary antibodies dissolved in TBSSM buffer (16 h at 4 °C), and washed three times with TBS buffer containing 0.05% Tween 20. Horseradish peroxidase-coupled secondary antibodies dissolved in TBSSM buffer were applied to the membranes (1 h at room temperature), which were then washed again three times, incubated in 2 ml of SuperSignal reagent (Pierce), and observed using the LAS system (Fuji). To detect polyubiquitinated p180 in tsFT20 cells, 6% SDS-PAGE was used and Western blot analysis was carried out using a monoclonal anti-polyubiquitin antibody (FK2, Nippon Biotest Laboratory).

Co-immunoprecipitation Analysis—To detect polyubiquitinated p180, 1×10^7 tsFT20 cells were harvested after incubation for 9 h at 39.5 °C in the presence of 2 mM MG132. Cells were extracted with CSK/Triton X-100 buffer for 20 min at 4 °C and the detergent-resistant fraction was separated by centrifugation (10,000 × *g* for 5 min). The remaining pellet was mixed with CSK/Triton X-100 buffer and sonicated well by handy sonic UR-20P (TOMY SEIKO Inc. Japan). One mg of extract was mixed with 3 μl of anti-p180 antiserum for 16 h at 4 °C. Each sample was mixed with 20 μl of Protein G-Sepharose for 2 h at 4 °C and the unbound fraction was separated by centrifugation (10,000 × *g* for 2 min). The remaining pellet was washed with CSK/Triton X-100 buffer, dissolved in 30 μl of SDS sample buffer, and subjected to SDS-PAGE and Western blot analysis using polyclonal anti-p180 antibody and monoclonal anti-polyubiquitin antibody.

Immunofluorescence Microscopy—Eight-well chamber slides were pre-treated with poly-L-lysine (1 mg/ml) for 2 h at 37 °C and 3×10^4 cells were seeded per well and incubated for 16 h at 37 °C. The cells were transfected as described above and incubated for 48 h at 33 °C. Inhibitors were applied either separately or in combination as described above and the cultures were incubated for another 1 h at 33 °C. The cells were then either shifted to 39.5 °C or kept at 33 °C as a control. Cell fixing, staining with anti-p180, anti-p68, and anti-Mcm7 (Sigma) antibodies, and subsequent observation by fluorescence microscopy (Olympus, AX70) were done as previously described (14, 46). To increase the detection sensitivity and to eliminate the endogenous p180 signal, monoclonal anti-GFP antibodies (Sigma) were used for staining. In three independent experiments, a total of 600 cells was counted and localization of overexpressed protein was classified as nuclear, nuclear and cytoplasmic, or cytoplasmic. The direct GFP signal and the signal detected with anti-GFP antibodies were visualized as green and red, respectively. DNA was stained with Hoechst 33258 (blue). To detect endogenous p180 in tsFT20 cells, digital images were captured and processed with fluorescence microscopy and deconvolution analysis using a nearest neighbor method with HazeBuster software (VayTek, Inc.) (48). The stack images of 10 optical sections with a step size of 200 nm were then deconvolved in three dimensions. To visualize cytoplasm in FM3A cells, endogenous biotin in the mitochondria was labeled with Alexa Fluor 488 streptavidin (Invitrogen).

Time-lapse Fluorescence Microscopy—To observe living cells, 2.0×10^5 NIH3T3 cells in 2 ml of Dulbecco's modified Eagle's medium containing 10% calf serum were seeded in 35-mm dishes with a glass slide on the bottom and incubated for 16 h at 37 °C. The cells were transfected with 2.4 μg of $p180^{tsFT20}$GFP DNA, 1.6 μg of p68 DNA, 6 μl of transfectin, and 500 μl of serum-free media. After incubation for 48 h at 33 °C, the media was changed to CO_2-independent media and the temperature was up-shifted and kept constant at 39.5 °C using a microscope stage heater (Olympus, MI-IBC-I). To monitor $p180^{tsFT20}$GFP, cells were kept for 5 h at 39.5 °C, and the temperature was then reduced and maintained at 33 °C. The GFP signal was observed and pictures were taken every 6 or 10 min. For photoactivation experiments, cells expressing PA-GFP-tagged p180 or $p180^{tsFT20}$ were photoactivated by a 10-s exposure to 420 nm light (filter BP400–440, Olympus) from a shuttered 100-watt mercury epi-illuminator with a ×40 UPlanApo objective. Cells were co-transfected with monomeric RFP1-p68 to identify those expressing $p180^{tsFT20}$PA-GFP. Live cell images were acquired with a ×20 UPlanApo objective.

siRNA Depletion—Two rounds of siRNA oligonucleotide transfections were performed to reduce the expression level of p68. siRNA duplexes were transfected into NIH3T3 cells using siLentFect lipid reagent (Bio-Rad) according to the manufacturer's instructions. 20 pM duplex RNA was used for each transfection. The procedure was repeated on the second day, and cells were harvested on the fourth day. The following RNA oligonucleotides were used: control, 5′-UUCUCCGAACGUGUCACGUTT-3′; si68-1, 5′-CGGUAAAGCGAAA-

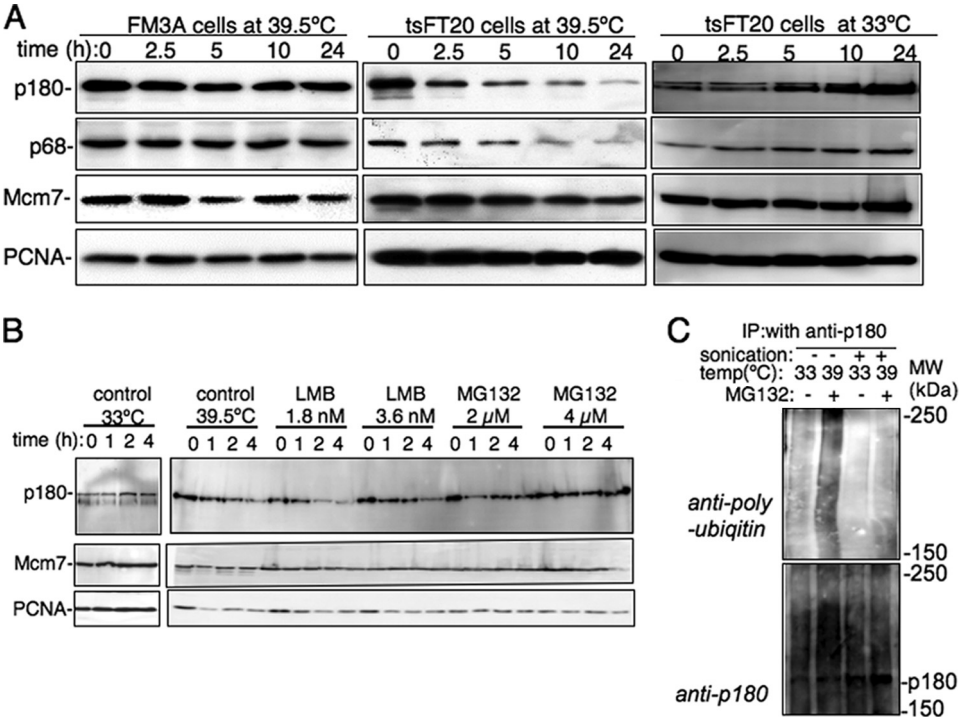

FIGURE 1. **Degradation of aberrant endogenous p180 in tsFT20 cells.** *A*, FM3A and tsFT20 cells were incubated at the restrictive or permissive temperatures for the indicated time, harvested, and lysed in SDS sample buffer. Twenty μg of whole cell extract was loaded on each lane and Western blot analysis was carried out using anti-p180, anti-p68, anti-Mcm7, and anti-proliferating cell nuclear antigen antibodies. *B*, tsFT20 cells were incubated in the presence of LMB (1.8 or 3.6 nM) or MG132 (1 or 2 μM) or without treatment at 33 or 39.5 °C for the indicated hours and protein levels of p180 were quantified by Western blot analysis. *C*, tsFT20 cells were incubated at 33 or 39.5 °C for 9 h in the presence or absence of 2 mM MG132, harvested, and fractionated into a soluble protein fraction (CSK+T solution without sonication (−), after sonication (+)). One-mg extracts were immunoprecipitated with anti-p180 antibody, and precipitates were loaded on a 6% acrylamide gel and Western blot analysis was carried out using anti-p180 antibody, and anti-polyubiquitin monoclonal antibody.

GGAUAATT-3′; si68-2, 5′-GAGAAGUUCUGACCAGUAATT-3′; si68-3, 5′-GAUUCAGCCGAGUCCUUAATT-3′; si68-4, 5′-CAGAGACAUUGUUUCUAUATT-3′.

RESULTS

Endogenous p180^{tsFT20} Is Degraded in the Nucleus at Restrictive Temperature and Expressed in the Cytoplasm—The temperature-sensitive mutant cell line tsFT20 is characterized by severe defects in cell cycle progression and DNA replication. These phenotypes were assigned to a single point mutation in the largest subunit of the mouse DNA polymerase α complex, p180. The properties of the respective protein (designated p180^{tsFT20}) have been studied on a biochemical level, but its expression levels, localization pattern, turnover rate, and nuclear transport properties remained unknown. For the intriguing possibility to use this protein variant as a tool to study protein quality control mechanisms specifically in the nucleus, we decided to look at the endogenous p180^{tsFT20} expression levels in the original tsFT20 cell line.

For that, FM3A wild-type cells and tsFT20 cells were incubated at 33 or 39.5 °C for 2–24 h, harvested by centrifugation, and lysed in SDS sample buffer. The cellular level of DNA polymerase α was monitored with anti-p180 and anti-p68 antibodies. Surprisingly, as shown in Fig. 1*A*, endogenous p180^{tsFT20} was rapidly degraded at the restrictive temperature, whereas the level of endogenous p180 in both FM3A wild-type cells at 39.5 °C and tsFT20 cells at 33 °C (permissive temperature) remained constant. Interestingly, the level of the second largest subunit, p68, also decreased similarly to that of p180, whereas the levels of Mcm7 and proliferating cell nuclear antigen (used as controls) did not change. Therefore, we concluded that endogenous p180^{tsFT20} is rapidly degraded upon temperature upshift in the tsFT20 cell line, concomitantly with the tightly associated p68 subunit. To define whether the disappearance of endogenous p180^{tsFT20} from the nucleus is dependent on nuclear export or the ubiquitin-mediated proteasome pathway, tsFT20 cells were incubated in the presence or absence of the nuclear export inhibitor LMB or the proteasome inhibitor MG132, and protein levels of p180^{tsFT20} were quantified by Western blot analysis (Fig. 1*B*). LMB showed no significant effect on the reduction of p180^{tsFT20}, whereas MG132 reduced the degradation of p180^{tsFT20}. This suggests that first, the CRM1-dependent nuclear export pathway is not involved in the degradation of endogenous p180^{tsFT20} and second, that the degradation of endogenous p180^{tsFT20} is dependent on the ubiquitin-mediated proteasome pathway and may be specifically in the nucleus. To verify ubiquitin-mediated degradation, proteasome function was inhibited by incubation with MG132 and samples were prepared for immunoprecipitation and Western blot analysis (Fig. 1*C*). One mg of protein from MG132-treated tsFT20 cells at the restrictive temperature was incubated with anti-p180 antiserum and Western blot was performed with a monoclonal anti-polyubiquitin antibody as shown in Fig. 1*C*. Interestingly, polyubiquitinated p180 was only observed in the soluble fraction of tsFT20 cell extracts at the restrictive temperature, and in the presence of MG132. In sonication-dependent insoluble fractions, p180 is clearly detectable, however, not in its polyubiquitinated form.

Cytoplasmic Localization of the p180^{tsFT20} Protein in tsFT20 Cells—To further examine whether endogenous p180^{tsFT20} is degraded in the nucleus or cytoplasm at the restrictive temperature, tsFT20 cells were stained with anti-p180 antibodies. For visualizing the cytoplasm in tsFT20 cells, endogenous biotin in the mitochondria was stained with Alexa Fluor 488-streptavidin and deconvolution imaging performed. We found that endogenous p180^{tsFT20} was exclusively localized in the nucleus at the permissive temperature, whereas surprisingly, p180^{tsFT20} accumulated in the cytoplasm at the restrictive temperature (Fig. 2*A*). Importantly, the observed specificity for cytoplasmic localization occurred even despite a rapid decrease of the overall

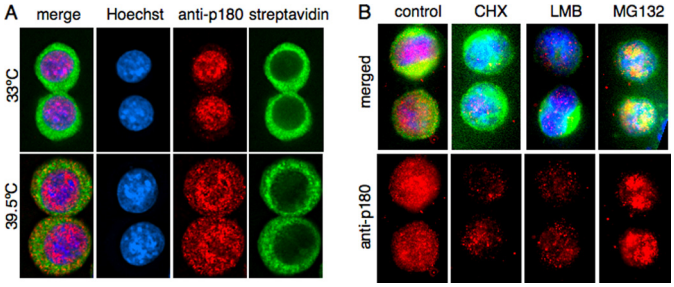

FIGURE 2. **Immunofluorescent staining of aberrant endogenous p180 in tsFT20 cells.** *A*, tsFT20 cells were cultured on poly-L-lysine-coated slide chambers and incubated at 33 or 39.5 °C for 10 h. Endogenous p180 mutant was detected with anti-p180 antibody, endogenous biotin in mitochondria was visualized by Alexa Fluor 488-conjugated streptavidin and DNA was stained with Hoechst 33258. Images were deconvoluted using Hazebuster software as described under "Experimental Procedures." *B*, tsFT20 cells were incubated for 5 h at 39.5 °C in the presence of 2 μM cycloheximide or 6.8 nM LMB, or 2 μM MG132. Endogenous p180^{tsFT20} was detected with anti-p180 antibodies, endogenous biotin in mitochondria was visualized by Alexa Fluor 488-conjugated streptavidin, and DNA was stained with Hoechst 33258.

p180^{tsFT20} level (Fig. 1*A*). To test the dependence of cytoplasmic accumulation of aberrant endogenous p180^{tsFT20} on protein synthesis, nuclear export, and proteasome-dependent degradation, tsFT20 cells were incubated in the presence of various inhibitors (Fig. 2*B*). In the presence of the protein synthesis inhibitor CHX, cytoplasmic expression of p180 was clearly decreased, indicating that the accumulation of cytoplasmic p180^{tsFT20} in the absence of CHX is newly synthesized p180. In the presence of the proteasome inhibitor MG132, most of the signal remained in the nucleus p180. Interestingly, aggregates of aberrant proteins that cannot be degraded by the proteasome are only visible in the nucleus. In the presence of leptomycin B, a nuclear export inhibitor, the overall effects concerning protein expression (Fig. 1*B*) and subcellular staining of p180^{tsFT20} (Fig. 2*B*) are milder, indicating that nuclear export mechanisms are not a major cause of the observed cytoplasmic accumulation. Taken together, these results suggested that clearance of aberrant endogenous p180^{tsFT20} from the nucleus at the restricted temperature is mainly due to proteasome-dependent degradation, whereas its cytoplasmic expression is due to *de novo* protein synthesis.

Transient Expression of p180^{tsFT20} in Mammalian Cultured Cells—To confirm and extend our results on endogenous p180^{tsFT20} and get a clearer picture on the mechanisms that exclude aberrant p180^{tsFT20} from the nucleus, we transiently expressed p180 (WT and p180^{tsFT20}) in mammalian cultured cells (supplemental Fig. S1*A*).

All constructs were expressed at the expected molecular weights and at similar levels (supplemental Fig. S1*B*). Co-transfection with a plasmid encoding the second largest subunit of the DNA polymerase α complex, the p68 protein, strongly increased the expression of p180 (14) and p180^{tsFT20}, independent of the presence of the GFP tag. These results indicate that like wild-type p180, the level of newly synthesized p180^{tsFT20} increases in the presence of p68. The more rapidly migrating p180 and p180GFP bands are due to amino-terminal degradation of full-length p180, as described previously (14). Moreover, temperature up-shift decreased the expression level of p180GFP and p180^{tsFT20}GFP (data not shown; Fig. 3*D*), however, NH_2- and COOH-terminal truncated variants of His-tagged p180, designated H-core and H-core^{tsFT20}, showed constant expression in the presence and absence of p68 (supplemental Fig. S1*B*). Because p68 associates with the COOH-terminal region of p180, the presence of p68 had no effect on H-core expression, as previously described (14). The finding also raises a model in which p180 is degraded via degron motifs in the COOH terminus that can be covered via association with p68.

Nuclear Exclusion of Transiently Expressed Aberrant p180^{tsFT20} Protein—To determine the subcellular localization of transiently expressed p180GFP and p180^{tsFT20}GFP, NIH3T3 cells were transfected with plasmids in the presence or absence of the p68 expression construct. The cells were seeded in 8-well chamber slides and incubated for 48 h at 33 °C to assure full protein expression. The temperature was then shifted to 39.5 °C or kept at 33 °C as a control, and the cells were fixed and observed by immunofluorescence microscopy. For protein detection, we monitored the direct GFP signal and also used polyclonal anti-p180 antibodies that could be visualized with Alexa 594-labeled secondary antibodies. In cells that were not transfected with the p180GFP or p180^{tsFT20}GFP constructs, anti-p180 antibodies did not produce a signal under these conditions (data not shown).

At permissive temperature, both wild-type p180GFP and mutant p180^{tsFT20}GFP clearly localized in the nucleus of mouse NIH3T3 cells in the presence of ectopically expressed p68 protein (supplemental Fig. S2, *A* and *C*). At restrictive temperature in the presence of p68, the wild-type protein remained in the nucleus, whereas the mutant form was found exclusively in the cytoplasm (supplemental Fig. 2, *B* and *C*). We confirmed these results in COS-1 cells (data not shown). In the absence of transiently expressed p68, both p180GFP and p180^{tsFT20}GFP exclusively localized in the cytoplasm, thus confirming the essential role of the p68 protein in nuclear entry of the p180 protein (supplemental Fig. S2, *A*–*C*) (14). Cell counting experiments revealed that these correlations are very specific. For each condition, more than 150 transfected cells were observed and the staining pattern was categorized as nuclear or cytoplasmic (supplemental Fig. S2*C*). Notably, in the case of p180^{tsFT20}GFP co-expressed with p68, we found that more than 80% of transfected cells exhibited nuclear fluorescence at the permissive temperature, whereas after incubation for 16 h at the restrictive temperature, the protein was expressed in the cytoplasm in more than 95% of transfected cells.

For comparison, we determined the localization pattern of the p180 H-core constructs. As expected, H-core proteins with or without the tsFT20-specific point mutation were expressed exclusively in the cytoplasm at 33 °C as well as at 39.5 °C, independent of the presence of p68 (supplemental Fig. S2*D*). Thus, these truncated proteins exhibited a localization pattern identical to that of p180^{tsFT20}GFP at the restrictive temperature.

To eliminate the possibility that the GFP tag affects the subcellular distribution of p180^{tsFT20}GFP, we monitored the exogenous expression of untagged protein in NIH3T3 cells by immunostaining with anti-p180 antibodies. Consistent with the experiments in which the GFP-tagged constructs were used, untagged p180 entered the nucleus at the permissive temperature in the presence of p68, whereas the p180^{tsFT20} protein

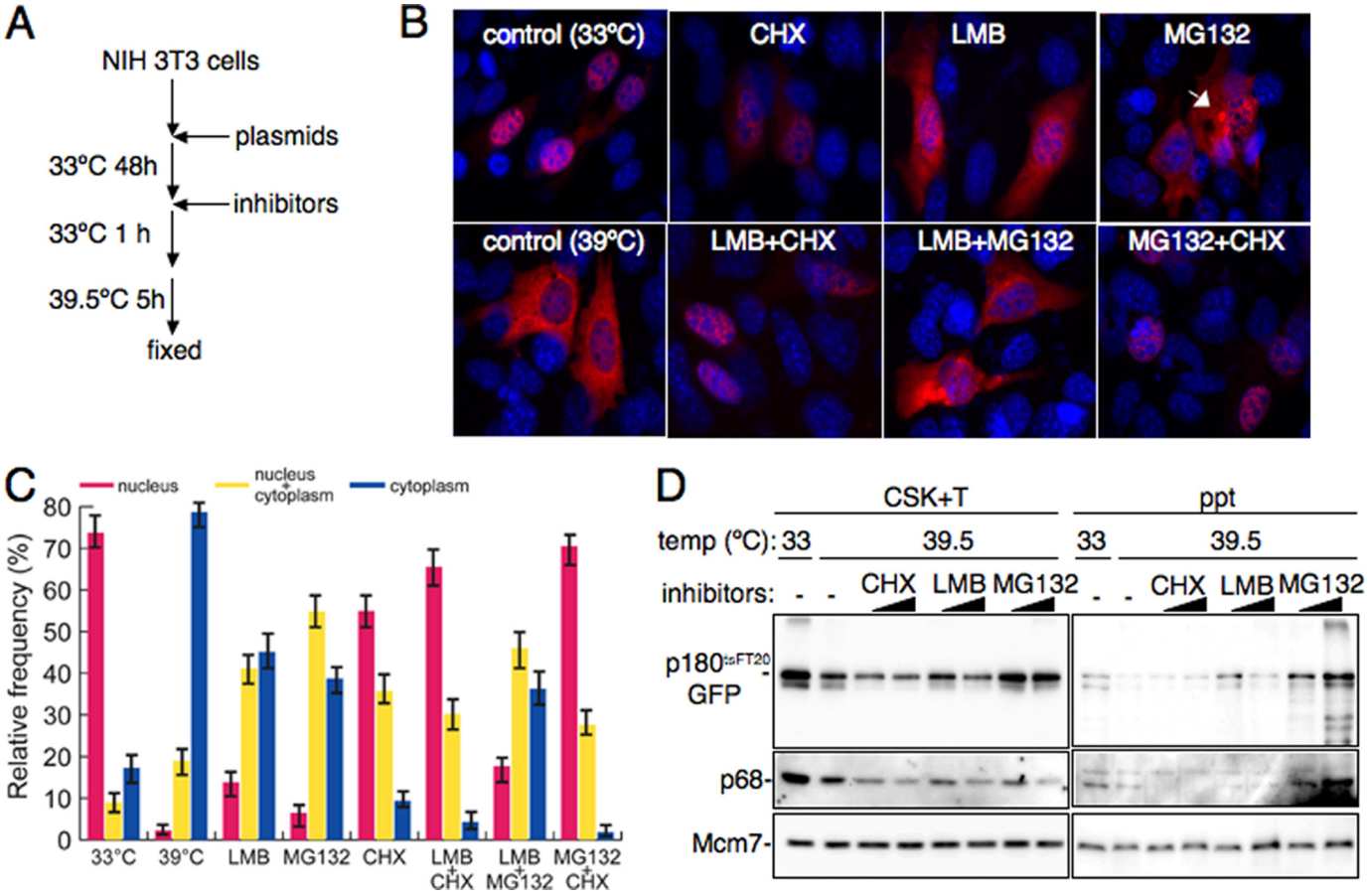

FIGURE 3. **Effects of inhibitors on the subcellular localization of the p180^{tsFT20}GFP variant.** *A*, experimental protocol. Cells were transfected with p180^{tsFT20}GFP and p68 and incubated for 48 h at 33 °C. After the addition of inhibitors, cells were incubated for another hour before the temperature was shifted to 39.5 °C for 5 h and cells were finally fixed and observed. *B*, representative staining patterns of treated cells. The GFP signal was detected using anti-GFP and Alexa-coupled secondary antibodies and is shown in *red*. The nucleus was stained with Hoechst 33258 showing a *blue* color. The *arrow* indicates aggresome formation. *C*, statistical evaluation. Six hundred cells from three independent experiments were counted, and staining patterns were classified: nucleus, nucleus and cytoplasm, and cytoplasm. The mean ± S.D. of three experiments are shown in the figure. *D*, Western blot analysis of various samples. The soluble protein fraction S1 (*CSK+T*) and the pellet fraction (*ppt*) of lysates from COS-1 cells transfected with p180^{tsFT20}GFP and p68 were subjected to SDS-PAGE and Western blot analysis was carried out using polyclonal anti-p180 and anti-p68 antibodies. The inhibitors CHX, LMB, and MG132 were applied at concentrations of 33 μM and 0.1 mM, 2.3 and 6.8 nM, and 0.67 and 2 μM, respectively. Mcm7 was detected with anti-Mcm7 antibodies as a loading control.

was found exclusively in the cytoplasm (data not shown), thus indicating that the GFP tag has no effect on the observed phenotype.

Accumulation of p180^{tsFT20}GFP in the Cytoplasm Is Rapid, Temperature-dependent, and Reversible—To further investigate the changes in the intracellular localization of p180^{tsFT20}GFP after temperature up-shift, we carried out time-lapse fluorescence microscopy analysis. Therefore, NIH3T3 cells transfected with p180^{tsFT20}GFP and p68 were cultured for 48 h at 33 °C. The temperature was then shifted to 39.5 °C, kept constant using a stage heater apparatus, and the GFP signal was monitored by taking a picture every 10 min. These observations indicated that the transition from nuclear to cytoplasmic expression was complete after less than 5 h (supplemental Fig. S3*A* and Movie 1). The protein began to accumulate in the cytoplasm a few minutes after the temperature shift, significantly increased during the first 3 h, and then reached a plateau. Instead, wild-type p180GFP showed stable nuclear expression in control experiments (data not shown).

Next, to test whether the mutation-specific accumulation of p180^{tsFT20}GFP in the cytoplasm is reversible, we observed cytoplasmically stained cells after incubation for 5 h at 39.5 °C, lowered the temperature back to 33 °C, and quantified the signal every 6 min. Nuclear entry rapidly occurred, and most of the p180^{tsFT20}GFP protein was found in the nucleus within 1 h (supplemental Fig. S3*B* and Movie 2).

Alterations in p180^{tsFT20}GFP Localization Involve de Novo Synthesis, Nuclear Degradation, and Export—Next, we wanted to gain further insights into the mechanisms that cause the changes in temperature-dependent localization of aberrant p180^{tsFT20}. Therefore, cells expressing p180^{tsFT20}GFP in the presence of p68 were treated with specific inhibitors such as CHX, LMB, and MG132. For this, NIH3T3 cells were co-transfected with p180^{tsFT20}GFP and p68 and incubated for 48 h at 33 °C (Fig. 3*A*). The cells were incubated with inhibitors for 1 h, shifted to 39.5 °C for 5 h, fixed, and stained. To overcome the cytotoxicity of LMB and MG132, we seeded NIH3T3 cells at higher concentrations (3×10^4 cells/well) in 8-well chamber slides in which the wells were pre-treated with poly-L-lysine for 2 h at 37 °C. To avoid detecting endogenous p180 and to increase the sensitivity to GFP-tagged proteins, we used monoclonal anti-GFP antibodies in combination with Alexa 594-la-

beled secondary antibodies. Inhibitors were applied either singly or doubly. For each condition, 600 transfected cells from each of three independent experiments were counted and the staining pattern was classified as nuclear, nuclear and cytoplasmic, or cytoplasmic (Fig. 3, *B* and *C*).

CHX generally inhibits protein synthesis by blocking the peptidyltransferase in the large ribosomal subunit of mammalian cells. Its addition, prior to the shift to restrictive temperature, prevented the cytoplasmic expression of p180^{tsFT20}GFP, whereas the level of nuclear protein decreased continuously but was still visible after 5 h. Therefore, the strong staining of cytoplasmically localized p180^{tsFT20}GFP at the restrictive temperature apparently derives from newly synthesized protein. The application of LMB, a CRM1-dependent nuclear export inhibitor, shows some effect by increasing the proportion of the nuclear-stained fraction. This observation argues that in the absence of LMB, CRM1-sensitive export mechanisms are to some degree involved in the reduction of nuclear p180^{tsFT20}GFP levels after a temperature shift to 39.5 °C. The peptide aldehyde MG132 is a proteasome substrate analogue that specifically inhibits proteasome-dependent protein degradation. When applied to cells expressing p180^{tsFT20}GFP, it caused the mutant protein to persist in the nucleus, and changes in the nuclear expression pattern were correlated with aggresome formation in the cytoplasm and enrichment in the ER or ER-associated compartments (Fig. 3*B*). Notably, as the overall level of p180^{tsFT20} increased after MG132 treatment, we suggest that under normal conditions, proteasome-dependent mechanisms are involved in the degradation of mutant p180^{tsFT20} in the nucleus and cytoplasm.

To confirm these inhibitory effects, we tested combinations of the compounds following the same protocol (Fig. 3*A*). Indeed, when CHX was included with LMB or MG132, the cytoplasmic expression of p180^{tsFT20}GFP remained low and the number of cells exhibiting nuclear staining increased dramatically compared with that of untreated cells and increased slightly compared with that of cells treated only with CHX. Thus, CHX again clearly inhibited *de novo* protein synthesis in the cytoplasm, whereas LMB and MG132 both increased the fraction of cells with nuclear staining. When MG132 and LMB were applied together, the number of treated cells exhibiting nuclear staining was greater than that of untreated cells. However, there was no significant difference in these frequencies with respect to cells treated with either MG132 or LMB alone. Therefore, MG132 and LMB seem to affect the same protein fraction, and the export and degradation processes might be linked. Comparison of CHX-treated cells with those treated with both CHX and LMB reveals that LMB might inhibit the expression of a small fraction of cytoplasmically localized protein that is visible when only CHX but not LMB was applied. This fraction may represent exported protein.

The effect of each inhibitor was further examined by Western blot analysis using COS-1 cells (Fig. 3*D*). The soluble protein fraction containing free proteins from the cytoplasm and the nucleus (CSK+T) and the pellet protein fraction containing proteins bound to nuclear structures and aggregates (ppt) were analyzed. The results of this experiment confirmed that CHX significantly reduces the level of free protein, whereas MG132

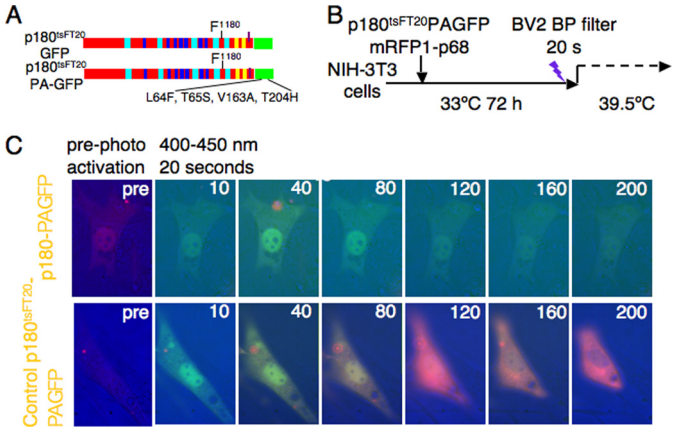

FIGURE 4. **Photoactivation of PA-GFP-tagged p180^{tsFT20} in NIH3T3 cells.** *A*, constructs of p180^{tsFT20}PA-GFP are depicted. Four amino acid residues in GFP were changed as described (47). *B*, experimental protocol. Cells were transfected with p180^{tsFT20}PA-GFP and p68 and incubated for 48 h at 33 °C. After photoactivation, cells were incubated at the restrictive temperature and images of live cells were acquired. *C*, photoactivation of p180-PA-GFP and p180^{tsFT20}PA-GFP. NIH3T3 cells expressing p180^{tsFT20}PA-GFP or p180-PA-GFP together with mRFP1-p68 were irradiated with 400–440 nm light for 20 s and live cell imaging after photoactivation was conducted. PA-GFP fluorescence was not observed before photoactivation. The time after the temperature shift is indicated in minutes, exposure times for mRFP1 and GFP were 0.1 and 1 s, respectively.

treatment results in an increase of this fraction due to the inhibition of proteasome-dependent degradation. LMB treatment also led to a slight decrease in free protein expression when applied in higher concentrations. Regarding the pellet fraction, CHX and LMB had no significant effect, whereas MG132 treatment causes a dramatic increase in p180^{tsFT20}GFP, which is presumably complexed with the similarly abundant p68. The smeared band of higher migrating bands may represent ubiquitinated p180^{tsFT20} protein variants.

Based on the findings on endogenous and transiently expressed p180^{tsFT20}, we concluded that the turnover of p180^{tsFT20}GFP (namely, its exclusion from the nucleus) after a temperature shift to 39.5 °C may be separated into two distinct processes: first, the mutant protein is rapidly synthesized *de novo* in the cytoplasm but, at the restrictive temperature, is unable to enter the nucleus due to a mutation-specific, temperature-sensitive effect. Second, nuclear-localized protein is degraded in a proteasome-dependent manner in the nucleus and to a minor extent in the cytoplasm after export from the nucleus.

Spatial and Temporal Monitoring of a Photoactivatable Version of GFP-tagged p180^{tsFT20}PA-GFP—To further distinguish the relative contributions of protein degradation and de *novo* synthesis, experiments with photoactivatable GFP (PA-GFP) were performed. PA-GFP has been developed recently as a GFP variant that fluoresces only after irradiation with 400–440 nm light, allowing for the selective induction of fluorescence at a desired site and time (47). We constructed a PA-GFP-tagged version of p180^{tsFT20} (Fig. 4*A*) to monitor the nuclear-localized protein at the restrictive temperature and carried out the experiments as indicated in Fig. 4*B*. NIH3T3 cells were then transfected with p180^{tsFT20}PA-GFP and p68-mRFP1 and incubated for 72 h at the permissive temperature. The cells were co-transfected with p68-mRFP1 to label transfected cells (49). As shown

in Fig. 4*C*, fluorescence of p180^{tsFT20}PA-GFP was undetectable before photoactivation in NIH3T3 cells but could be observed upon irradiation with 400–440 nm light and time-lapse images were acquired at the restrictive temperature. Photoactivated GFP signals gradually decreased equally in the nucleus and the cytoplasm and can be detected until 200 min after photoactivation under these conditions (Fig. 4*C* and supplemental Movie 3). As a control, photoactivated p180^{tsFT20}PA-GFP was visualized in the nucleus, where the fluorescent intensity also decreased gradually (supplemental Movie 4). Furthermore, the cytoplasmic fraction of p180^{tsFT20} was still observed 200 min after the up-shift to the restrictive temperature, whereas nuclear p180^{tsFT20} is totally removed from the nucleus, indicating degradation of aberrant DNA polymerase α in the nucleus. As the cytoplasmic staining remained rather constant throughout the time course, these results are in accordance with the conclusions that most of the nuclear-localized p180^{tsFT20} is rapidly degraded in the nucleus at the restrictive temperature and that the cytoplasmic p180^{tsFT20} seen at the restrictive temperature is mainly due to *de novo* protein synthesis.

Temperature-dependent Interaction between p180^{tsFT20} and p68—Based on the results obtained from the immunofluorescence experiments in NIH3T3 cells (supplemental Fig. S2, *A* and *B*), we considered that the mutation in p180^{tsFT20} leads to conformational changes affecting its COOH-terminal domain. These alterations could result in an inability to bind the smaller p68 subunit and a subsequent defect in the nuclear entry. Indeed, wild-type p180GFP protein in the absence of p68 as well as wild-type H-core protein lacking the p68 binding site, were both exclusively localized in the cytoplasm (supplemental Fig. S2, *A*, *B*, and *D*). To test whether failure of newly synthesized p180^{tsFT20}GFP protein to bind p68 causes its accumulation in the cytoplasm, we carried out co-immunoprecipitation experiments. Therefore, we co-expressed p180GFP or p180^{tsFT20}GFP with p68 and then precipitated the p180-associated p68 from cell lysates using anti-GFP antibodies. This experiment showed that although both p180GFP and p180^{tsFT20}GFP interact with p68 at the permissive temperature, the amount of p68 co-precipitating with p180^{tsFT20}GFP was significantly reduced at the restrictive temperature (Fig. 5*A*), suggesting that the binding capacity of p180^{tsFT20}GFP to p68 is weakened under these conditions. To further examine the effect of temperature up-shift on the interaction between p180^{tsFT20} and p68, immunoprecipitated complexes containing p180^{tsFT20} and p68, which were expressed at the permissive temperature, were incubated for 1 h at 39.5 or 4 °C, and associated p68 was then detected by Western blot analysis. As shown in Fig. 5*B*, both p180 and p180^{tsFT20} associated with p68 at 39.5 or 4 °C, suggesting that once p68 and p180^{tsFT20} bind at the permissive temperature, the heterodimer is stable even at the restrictive temperature. We should note here that the amounts of p68 retained at 39.5 °C are significantly lower than those at 4 °C, even for the wild-type p180 subunit, probably because the interaction between p180 and p68 is less strong at 39.5 °C, especially when the p180 subunit is bound to the anti-p180 antibody. Taken together, the reduced level of p68 complexed with p180^{tsFT20}GFP at the restrictive temperature as shown in Fig. 5*A* might be caused by the inability of newly synthesized p180^{tsFT20}GFP to bind p68 rather than to the dissociation of pre-existing p180^{tsFT20}-p68 heterodimers. We conclude that the p180^{tsFT20} mutation leads to conformational changes that prevent newly synthesized p180^{tsFT20} from binding p68, thus causing the subsequent defect in nuclear entry.

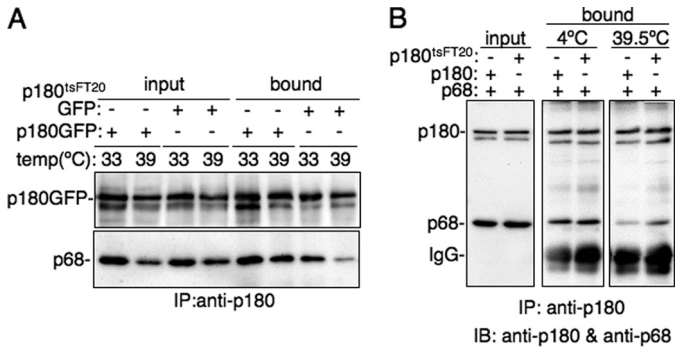

FIGURE 5. **Temperature-dependent interaction between p180^{tsFT20} and p68.** *A*, interaction between p180GFP or p180^{tsFT20}GFP and p68 at permissive and restrictive temperatures. After incubation at the respective temperatures for 5 h, lysates of COS-1 cells transfected with p180GFP or p180^{tsFT20}GFP in the presence of p68, and p180GFP or p180^{tsFT20}GFP were precipitated with 2 μl of monoclonal anti-GFP antibodies in 50 μl of CSK buffer containing Triton X-100 and mixed with protein G-Sepharose beads. The precipitate was subjected to Western blot analysis using polyclonal antibodies against p180 and p68. Input samples refer to COS-1 cell lysates before immunoprecipitation (*IP*), whereas the bound fraction represents samples obtained from the precipitate. *B*, p68 and p180 or p180^{tsFT20} co-expressed in COS-1 cells at the permissive temperature were immunoprecipitated with anti-p180 antibodies, washed with CSK buffer, and incubated *in vitro* for 1 h at 4 or 39.5 °C. The remaining fractions of bound p68 as well as p180 or p180^{tsFT20} in the precipitates were detected by Western blot analysis. *IB*, immunoblot.

Depletion of Endogenous p68 by siRNA Causes a Decrease of Overall Endogenous p180 Protein but Specific Accumulation of Cytoplasmic p180—Previously, we reported that p68 facilitates both production and nuclear translocation of p180 (14). We showed that overexpressed p68 stabilizes p180 expression at the post-transcriptional level and in addition activates the nuclear localization signal of p180 at the COOH-terminal region. As all these data were based on a transiently transfected cDNA expression system, we want to confirm the roles of p68 in p180 expression and localization at the physiological level by depleting p68 with siRNA oligonucleotides. Four different oligonucleotides were designed and transfected into NIH3T3 cells. As shown in Fig. 6, *A* and *B*, the expression level of p68 was reduced after two rounds of transfection with three of four siRNAs revealed by Western analysis (si68-2, -3, and -4). Interestingly, the overall protein level of p180 is also decreased by depletion of p68, whereas the expression levels of Mcm7 and proliferating cell nuclear antigen are not altered. Next, to examine whether p180 localization is affected by depletion of p68, immunofluorescence analysis was performed. NIH3T3 cells were transfected with siRNAs, fixed with formaldehyde, and stained with anti-p180 and anti-p68 antibodies. Transfection with the control oligonucleotide exhibited nuclear localization of p180 and nuclear and cytoplasmic localization of p68. When siRNAs were introduced into NIH3T3 cells, the immunofluorescence signal of p68 could be reduced successfully. In conjunction with the depletion of p68, the localization pattern of p180 changed from nuclear to cytoplasmic expression. Taken together, these results indicate that endogenous p68 indeed ensures stable expression and nuclear localization of p180.

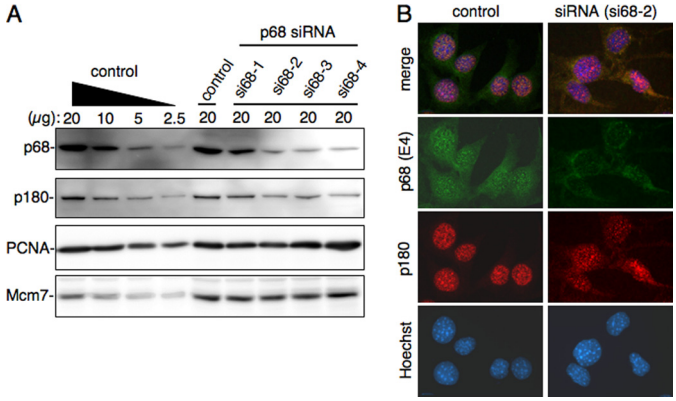

FIGURE 6. **Effect of RNA interference-mediated depletion of p68 on endogenous p180 expression and localization.** *A*, NIH3T3 cells were transfected with control or four different oligonucleotides designed to deplete p68. Transfection was repeated once after 24 h. Cells were then harvested 48 h after siRNA transfection, and proteins were extracted with CSK buffer containing Triton X-100. An extract with control oligonucleotides was serially diluted to compare the expression levels. Western analysis was carried out with anti-p180, anti-p68, anti-proliferating cell nuclear antigen (*PCNA*), and anti-Mcm7 antibodies. *B*, subcellular distribution of p180 in p68-depleted NIH3T3 cells was observed by immunofluorescence analysis. Cells were transfected with p68 siRNA twice and fixed 48 h after transfection. Endogenous p180 and p68 were detected by anti-p180 polyclonal and anti-p68 monoclonal antibodies (E4 (54)), DNA was stained with Hoechst 33258.

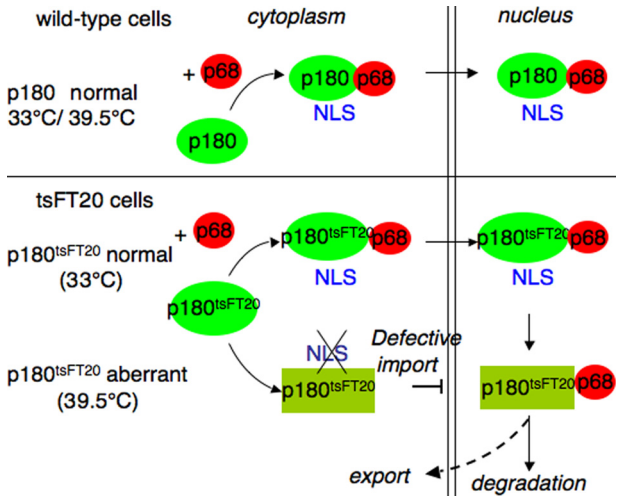

FIGURE 7. **Quality control mechanisms lead to the exclusion of aberrant p180 from the nucleus.** The clearance of non-functional p180 seems to result from two distinct concepts: nuclear entry defects of cytoplasmic protein and proteasome-dependent degradation in the nucleus. The DNA polymerase α p180 subunit enters the nucleus via its exposed nuclear localization signal in complex with the smaller p68 subunit at the permissive and restrictive temperatures and is expressed stably in the nucleus. The temperature-sensitive mutant form $p180^{tsFT20}$ has a phenotype comparable with that of the wild-type form at the permissive temperature. At the restrictive temperature, presumably due to an impaired binding to p68 and consequently inhibited nuclear localization signal exposure, newly synthesized mutant p180 accumulates in the cytoplasm, whereas nuclear-localized mutant protein is directly degraded, both in the nucleus as well as to a smaller extent in the cytoplasm after export.

Moreover, the subcellular localization of p68 has not been characterized so far. As we previously detected small amounts of monomeric p68 in NIH3T3 cells by glycerol density gradient sedimentation (46), the cytoplasmic expression of p68 observed in this study may represent an excess of its monomeric form.

DISCUSSION

Quality Control of DNA Polymerase α Is Crucial for Maintaining Genome Integrity—Several lines of evidence suggest that the quality of DNA polymerase α is critical for maintaining genome integrity. First, we previously found that tsFT20 cells transiently cultured at the restrictive temperature showed general and massive chromosomal aberrations, including chromatid gaps and breaks, chromosome pulverizations, and ring chromosomes (23). Second, tsFT20 cells cultured at the semi-permissive temperature exhibited alterations of telomeric DNA and chromatin structure (50). Third, in yeast cells with reduced protein levels of DNA polymerase α, highly elevated frequencies of chromosome translocations and chromosome loss was observed (35). Thus, the protein level as well as integrity of DNA polymerase α must be accurately controlled to avoid genome instability. In this report, we show that control systems for DNA polymerase α exist to ensure its proper quality in the nucleus.

Aberrant $p180^{tsFT20}$ Is Excluded from the Nucleus—As protein control mechanisms regulating the fate of aberrant proteins are largely unknown in the nucleus, we decided to look at p180 as a central nuclear component of the DNA polymerase α complex. We took advantage of a p180 variant harboring a point mutation that results in phenotypes specifically upon temperature up-shift to the restrictive temperature. Unexpectedly, we found that endogenous as well as transiently overexpressed $p180^{tsFT20}$ strictly localizes to the cytoplasm at the restrictive temperature and is excluded from the nucleus. We therefore defined $p180^{tsFT20}$ as a suitable model substrate that is prone to detection by nuclear quality control mechanisms. In the tsFT20 cell line, $p180^{tsFT20}$ is the only source of p180 at the restrictive temperature and therefore deleterious for the cells. However, it is very likely that in wild-type cells, those p180 molecules that are misfolded and show aberrant structures are cleared from the nucleus by the same mechanisms. Notably, such mechanisms seem to occur in two different compartments, at the nuclear entry step in the cytoplasm as well as via degradation in the nucleus (Fig. 7).

Control Mechanisms for Nuclear Entry—Time-lapse observation of living cells and the effects of treatments with different inhibitors suggested that following a temperature up-shift to 39.5 °C, *de novo* synthesized $p180^{tsFT20}$GFP protein is sequestered in the cytoplasm. We could show in several experiments in this and previous studies that the smaller DNA polymerase α subunit p68 is crucial for this observation. First, newly synthesized $p180^{tsFT20}$GFP is significantly impaired in binding p68 at the restrictive temperature (Fig. 5*A*). Second, the reduction of p68 by RNA interference resulted in a specific increase of p180 in the cytoplasm (Fig. 6*B*). Third, we previously found that transiently expressed p180 exclusively localizes in the cytoplasm in the absence of concomitant p68 overexpression (14). Thus, we conclude that the accumulation of $p180^{tsFT20}$ in the cytoplasm is due to conformational changes and a subsequent inability to bind p68, which finally results in a defective nuclear entry. This supports our conclusion that the nuclear localization of p180 is absolutely dependent on its interaction with p68, which specifically activates an nuclear localization signal in p180. These findings raise a model in which only properly folded and assem-

bled p180-p68 heterodimers enter the nucleus, thereby excluding aberrant proteins from nuclear import. We speculate that this mechanism is a common concept in cell biology to assure the stoichiometry and correct folding of multiprotein complex subunits in the nucleus.

Proteasome-dependent Degradation of Aberrant Nuclear Proteins—In addition to cytoplasmic sequestration of aberrant DNA polymerase α, the levels of nuclear-localized mutant protein decrease rapidly in a separate process apparently due to proteasome-dependent degradation in the nucleus. This is suggested by the findings that inhibition of proteasome-dependent degradation leads to aggresome formation in the nucleus, that nuclear endogenous $p180^{tsFT20}$ is degraded independently of nuclear export, and that experiments with PA-GFP tagged $p180^{tsFT20}$ exhibit degradation of nuclear-localized $p180^{tsFT20}$ in the nucleus at the restrictive temperature. Although proteasomes are also found in the nucleus (40, 41), degradation-mediated protein quality control in higher eukaryotic nuclei has not been demonstrated. Recently, it was reported that San1p-mediated degradation functions in quality control in yeast nuclei (45). San1 is a ubiquitin ligase that has exquisite specificity for aberrant proteins in the nucleus. The authors propose that San1-mediated degradation acts as the last line of proteolytic defense against the deleterious accumulation of improperly folded nuclear proteins. Thus, it is interesting to speculate that aberrant DNA polymerase α in mammalian nuclei is recognized by a similar protein quality control system finally leading to its clearance from the nucleus.

How Might Such Protein Control Mechanisms Work?—Aberrant nuclear proteins have to be at first recognized as being malformed (*e.g.* by chaperones due to exposed hydrophobic patches). Afterward, the malformed subunits have to be labeled with ubiquitin for protein degradation (mediated, *e.g.* by San1 in *S. cerevisiae* or chromatin immunoprecipitation and yet unknown E3 ligases in higher eukaryotes), extracted from a multisubunit complex (*e.g.* by Cdc48 in *S. cerevisiae* or p97 in higher eukaryotes), and finally delivered to nuclear proteasomes for degradation. Apart from this direct nuclear degradation, the exposition of normally hidden domains in aberrant proteins might directly lead to their recognition by the nuclear export machinery as a minor parallel pathway. Additionally, the nuclear entrance step demonstrates a quality control mechanism for DNA polymerase α in such a way that only intact p180-p68 heterodimeric complexes are permitted for nuclear entry, whereas newly synthesized aberrant DNA polymerase α is retained in the cytoplasm. This could indeed be a general mechanism, which holds true for other nuclear protein complexes. In such a model, only those proteins, which are fully expressed and able to form complexes with other subunits are capable for nuclear entry. If this stabilization by complex formation with other subunits does not occur, the protein is rapidly targeted for degradation in the cytoplasm. Especially for essential and accurately regulated proteins like proteins that are involved in DNA replication, such control mechanisms are of high value. Concerning other B-type DNA polymerases, DNA polymerase δ and ϵ both contain a second largest subunit similar to p68, which might have an analogous function in stabilization and nuclear entry of the largest subunit in the complex.

In this context, it is further interesting to note that in temperature-sensitive yeast Mcm10 mutants, depletion of Mcm10 during S phase results in degradation of DNA polymerase α without affecting other fork components (36). Thus, the nuclear expression level of DNA polymerase α may be tightly controlled at the nuclear entry step as well as by protein degradation in the nucleus, and Mcm10 may be directly involved in the quality control of DNA polymerase α. In addition, several further potential "substrates" (other than DNA polymerase α) of such control mechanisms have been mentioned in recent reports, thus underlining the biological significance of nuclear protein quality control. First, we believe that the phenomenon of nuclear exclusion of aberrant proteins does not only apply for DNA polymerase α, but also for other nuclear multisubunit complexes such as ORC, MCM, GINS, and other replicative or translesion DNA polymerases. In accordance, a recent paper (51) describes the protein stability of 8000 human proteins and found that cell cycle control categories including proteins in DNA replication are classified into a short-medium half-life group. Second, we believe that not only aberrant proteins but also basal proteins are recycled during cell cycle progression. Indeed, DNA polymerase β and λ are controlled by ubiquitination and degradation and seem to be very unstable proteins under basal conditions (52, 53). Such protein turnovers in the nucleus might be intimately linked with protein quality control mechanisms.

In summary, our results explain that many phenotypes associated with the original tsFT20 cell line, which are severely defective in DNA replication and cell cycle progression are probably due to the strict exclusion of aberrant $p180^{tsFT20}$ (the only source of p180 in these cells) from the nucleus. However, more importantly, our study suggests two distinct concepts of how the pool of malformed proteins in wild-type cells might generally be prevented from functioning inappropriately in the nucleus. First, in the cytoplasm, import of correctly folded subunits is assured by only allowing the import of protein complexes (as shown here for p180-p68 heterodimers). Second, proteasome-dependent degradation clears defective proteins in the nucleus. These mechanisms might very well hold true for assuring the functionality of other nuclear protein complexes.

Acknowledgments—We thank Dr. Masako Izumi and members of the Cellular Physiology and Cellular Dynamics Laboratories of RIKEN for helpful discussions, Drs. Roger Y. Tsien and Akihiko Nakano for mRFP1 cDNA, Dr. Jennifer Lippincott-Schwartz for kind comments on the usage of PA-GFP, Toshimasa Suzuki for technical assistance, and Yasue Ichikawa and Rie Nakazawa at the Bioarchitect DNA sequencing facility in RIKEN for DNA sequencing.

REFERENCES

1. Hubscher, U., Maga, G., and Spadari, S. (2002) *Annu. Rev. Biochem.* **71,** 133–163
2. Wang, T. S. (1991) *Annu. Rev. Biochem.* **60,** 513–552
3. Waga, S., and Stillman, B. (1998) *Annu. Rev. Biochem.* **67,** 721–751
4. Bell, S. P., and Dutta, A. (2002) *Annu. Rev. Biochem.* **71,** 333–374
5. Diede, S. J., and Gottschling, D. E. (1999) *Cell* **99,** 723–733
6. Dahlén, M., Sunnerhagen, P., and Wang, T. S. (2003) *Mol. Cell. Biol.* **23,** 3031–3042
7. Adams Martin, A., Dionne, I., Wellinger, R. J., and Holm, C. (2000) *Mol.*

Cell. Biol. **20,** 786–796
8. Qi, H., and Zakian, V. A. (2000) *Genes Dev.* **14,** 1777–1788
9. Grossi, S., Puglisi, A., Dmitriev, P. V., Lopes, M., and Shore, D. (2004) *Genes Dev.* **18,** 992–1006
10. Nakayama, Ji., Allshire, R. C., Klar, A. J., and Grewal, S. I. (2001) *EMBO J.* **20,** 2857–2866
11. Zhou, Y., and Wang, T. S. (2004) *Mol. Cell. Biol.* **24,** 9568–9579
12. Arezi, B., and Kuchta, R. D. (2000) *Trends Biochem. Sci.* **25,** 572–576
13. Foiani, M., Marini, F., Gamba, D., Lucchini, G., and Plevani, P. (1994) *Mol. Cell. Biol.* **14,** 923–933
14. Mizuno, T., Ito, N., Yokoi, M., Kobayashi, A., Tamai, K., Miyazawa, H., and Hanaoka, F. (1998) *Mol. Cell. Biol.* **18,** 3552–3562
15. Ekholm-Reed, S., Méndez, J., Tedesco, D., Zetterberg, A., Stillman, B., and Reed, S. I. (2004) *J. Cell Biol.* **165,** 789–800
16. Hua, X. H., Yan, H., and Newport, J. (1997) *J. Cell Biol.* **137,** 183–192
17. Ott, R. D., Rehfuess, C., Podust, V. N., Clark, J. E., and Fanning, E. (2002) *Mol. Cell. Biol.* **22,** 5669–5678
18. Voitenleitner, C., Rehfuess, C., Hilmes, M., O'Rear, L., Liao, P. C., Gage, D. A., Ott, R., Nasheuer, H. P., and Fanning, E. (1999) *Mol. Cell. Biol.* **19,** 646–656
19. Schub, O., Rohaly, G., Smith, R. W., Schneider, A., Dehde, S., Dornreiter, I., and Nasheuer, H. P. (2001) *J. Biol. Chem.* **276,** 38076–38083
20. Pearson, B. E., Nasheuer, H. P., and Wang, T. S. (1991) *Mol. Cell. Biol.* **11,** 2081–2095
21. Izumi, M., Yokoi, M., Nishikawa, N. S., Miyazawa, H., Sugino, A., Yamagishi, M., Yamaguchi, M., Matsukage, A., Yatagai, F., and Hanaoka, F. (2000) *Biochim. Biophys. Acta* **1492,** 341–352
22. Eki, T., Murakami, Y., Enomoto, T., Hanaoka, F., and Yamada, M. (1986) *J. Biol. Chem.* **261,** 8888–8893
23. Eki, T., Enomoto, T., Murakami, Y., Hanaoka, F., and Yamada, M. (1987) *Cancer Res.* **47,** 5162–5170
24. Eki, T., Enomoto, T., Murakami, Y., Miyazawa, H., Hanaoka, F., and Yamada, M. (1987) *Exp. Cell Res.* **171,** 24–36
25. Eki, T., Enomoto, T., Murakami, Y., Hanaoka, F., and Yamada, M. (1988) *Arch. Biochem. Biophys.* **260,** 552–560
26. Eki, T., Enomoto, T., Miyajima, A., Miyazawa, H., Murakami, Y., Hanaoka, F., Yamada, M., and Ui, M. (1990) *J. Biol. Chem.* **265,** 26–33
27. Ikehata, H., Kaneda, S., Yamao, F., Seno, T., Ono, T., and Hanaoka, F. (1997) *Mol. Cell. Biol.* **17,** 1484–1489
28. Izumi, M., Miyazawa, H., Harakawa, S., Yatagai, F., and Hanaoka, F. (1994) *J. Biol. Chem.* **269,** 7639–7644
29. Miyazawa, H., Tandai, M., Hanaoka, F., Yamada, M., Hori, T., Shimizu, K., and Sekiguchi, M. (1986) *Biochem. Biophys. Res. Commun.* **139,** 637–643
30. Murakami, Y., Yasuda, H., Miyazawa, H., Hanaoka, F., and Yamada, M. (1985) *Proc. Natl. Acad. Sci. U.S.A.* **82,** 1761–1765
31. Murakami, Y., Eki, T., Miyazawa, H., Enomoto, T., Hanaoka, F., and Yamada, M. (1986) *Exp. Cell Res.* **163,** 135–142
32. Pendergrass, W. R., Saulewicz, A. C., Hanaoka, F., and Norwood, T. H. (1994) *J. Cell. Physiol.* **158,** 270–276
33. Takada-Takayama, R., Hanaoka, F., Yamada, M., and Ui, M. (1991) *J. Biol. Chem.* **266,** 15716–15718
34. Yamaguchi, K., Kobayashi, M., Yamauchi, Y., Tanaka, A., Miyazawa, H., Izumi, M., and Hanaoka, F. (1995) *Cell Struct. Funct.* **20,** 285–291
35. Lemoine, F. J., Degtyareva, N. P., Lobachev, K., and Petes, T. D. (2005) *Cell* **120,** 587–598
36. Ricke, R. M., and Bielinsky, A. K. (2004) *Mol. Cell* **16,** 173–185
37. Zhu, W., Ukomadu, C., Jha, S., Senga, T., Dhar, S. K., Wohlschlegel, J. A., Nutt, L. K., Kornbluth, S., and Dutta, A. (2007) *Genes Dev.* **21,** 2288–2299
38. Richly, H., Rape, M., Braun, S., Rumpf, S., Hoege, C., and Jentsch, S. (2005) *Cell* **120,** 73–84
39. Ye, Y., Meyer, H. H., and Rapoport, T. A. (2001) *Nature* **414,** 652–656
40. Goldberg, A. L. (2003) *Nature* **426,** 895–899
41. Bennett, E. J., Bence, N. F., Jayakumar, R., and Kopito, R. R. (2005) *Mol. Cell* **17,** 351–365
42. Hershko, A., and Ciechanover, A. (1998) *Annu. Rev. Biochem.* **67,** 425–479
43. von Mikecz, A. (2006) *J. Cell Sci.* **119,** 1977–1984
44. Ward, C. L., Omura, S., and Kopito, R. R. (1995) *Cell* **83,** 121–127
45. Gardner, R. G., Nelson, Z. W., and Gottschling, D. E. (2005) *Cell* **120,** 803–815
46. Mizuno, T., Yamagishi, K., Miyazawa, H., and Hanaoka, F. (1999) *Mol. Cell. Biol.* **19,** 7886–7896
47. Patterson, G. H., and Lippincott-Schwartz, J. (2002) *Science* **297,** 1873–1877
48. Gorby, G. L. (1994) *J. Histochem. Cytochem.* **42,** 297–306
49. Campbell, R. E., Tour, O., Palmer, A. E., Steinbach, P. A., Baird, G. S., Zacharias, D. A., and Tsien, R. Y. (2002) *Proc. Natl. Acad. Sci. U.S.A.* **99,** 7877–7882
50. Nakamura, M., Nabetani, A., Mizuno, T., Hanaoka, F., and Ishikawa, F. (2005) *Mol. Cell. Biol.* **25,** 11073–11088
51. Yen, H. C., Xu, Q., Chou, D. M., Zhao, Z., and Elledge, S. J. (2008) *Science* **322,** 918–923
52. Parsons, J. L., Tait, P. S., Finch, D., Dianova, I. I., Allinson, S. L., and Dianov, G. L. (2008) *Mol. Cell* **29,** 477–487
53. Wimmer, U., Ferrari, E., Hunziker, P., and Hübscher, U. (2008) *EMBO Rep.* **9,** 1027–1033
54. Yagura, T., Kozu, T., Seno, T., and Tanaka, S. (1987) *Biochemistry* **26,** 7749–7754